Comparative efficacy of *Knema retusa* extract delivery *via* PEG-*b*-PCL, niosome, and their combination against *Acanthamoeba triangularis* genotype T4: characterization, inhibition, anti-adhesion, and cytotoxic activity

Siriphorn Chimplee[1], Watcharapong Mitsuwan[2,3,4], Masyitah Zulkifli[5], Komgrit Eawsakul[6,7], Tassanee Ongtanasup[6], Suthinee Sangkanu[8], Tooba Mahboob[9], Sonia M.R. Oliveira[10,11], Christophe Wiart[12], Siva Ramamoorthy[13], Maria de Lourdes Pereira[11,14], Shanmuga Sundar Saravanabhavan[15], Polrat Wilairatana[16] and Veeranoot Nissapatorn[8]

[1] School of Languages and General Education, Walailak University, Thasala, Nakhon Si Thammarat, Thailand
[2] Akkhraratchakumari Veterinary College, Walailak University, Thasala, Nakhon Si Thammarat, Thailand
[3] One Health Research Center, Walailak University, Thasala, Nakhon Si Thammarat, Thailand
[4] Center of Excellence in Innovation of Essential Oil, Walailak University, Thasala, Nakhon Si Thammarat, Thailand
[5] School of Pharmacy, University of Nottingham Malaysia Campus, Semenyih, Malaysia
[6] School of Medicine, Walailak University, Thasala, Nakhon Si Thammarat, Thailand
[7] Research Excellence Center for Innovation and Health Products (RECIHP), Walailak University, Thasala, Nakhon Si Thammarat, Thailand
[8] School of Allied Health Sciences, Southeast Asia Water Team (SEA Water Team), World Union for Herbal Drug Discovery (WUHeDD), and Research Excellence Center for Innovation and Health Products (RECIHP), Walailak University, Thasala, Nakhon Si Thammarat, Thailand
[9] Department of Pharmaceutical Biology, UCSI University, Kuala Lumpur, Malaysia
[10] Faculty of Dental Medicine, Catholic University, Viseu, Portugal
[11] CICECO-Aveiro Institute of Materials, University of Aveiro, Aveiro, Portugal
[12] The Institute for Tropical Biology and Conservation, University Malaysia Sabah, Jalan UMS, Kota Kinabalu, Sabah, Malaysia
[13] School of Bio Sciences & Technology, Vellore Institute of Technology (VIT), Velllore, India
[14] Department of Medical Sciences, University of Aveiro, Aveiro, Portugal
[15] Department of Biotechnology, Aarupadai Veedu Institute of Technology, Vinayaka Missions Research Foundation (DU), Chennai Campus, Paiyanoor, Chennai, India
[16] Department of Clinical Tropical Medicine, Faculty of Tropical Medicine, Mahidol University, Bangkok, Thailand

Submitted 12 April 2024
Accepted 14 October 2024
Published 15 November 2024

Corresponding author
Veeranoot Nissapatorn,
nissapat@gmail.com

Academic editor
Erika Braga

Additional Information and Declarations can be found on page 15

DOI **10.7717/peerj.18452**

ABSTRACT

Background. *Acanthamoeba* spp. is a waterborne, opportunistic protozoan that can cause amebic keratitis and granulomatous amebic encephalitis. *Knema retusa* is a native tree in Malaysia, and its extracts possess a broad range of biological activities. Niosomes are non-ionic surfactant-based vesicle formations and suggest a future targeted drug delivery system. Copolymer micelle (poly(ethylene glycol)-block-poly(ε-caprolactone); PEG-*b*-PCL) is also a key constituent of niosome and supports high stability and drug efficacy. To establish *Knema retusa* extract (KRe) loading in diverse nanocarriers *via* niosome, PEG-*b*-PCL micelle, and their combination and to study the effect of all

How to cite this article Chimplee S, Mitsuwan W, Zulkifli M, Eawsakul K, Ongtanasup T, Sangkanu S, Mahboob T, Oliveira SMR, Wiart C, Ramamoorthy S, Pereira ML, Saravanabhavan SS, Wilairatana P, Nissapatorn V. 2024. Comparative efficacy of *Knema retusa* extract delivery *via* PEG-*b*-PCL, niosome, and their combination against *Acanthamoeba triangularis* genotype T4: characterization, inhibition, anti-adhesion, and cytotoxic activity. *PeerJ* **12**:e18452 http://doi.org/10.7717/peerj.18452

types of nanoparticles (NPs) on *Acanthamoeba* viability, adherent ability, elimination of adherence, and cytotoxicity.

Methods. In this study, we characterized niosomes, PEG-*b*-PCL, and their combination loaded with KRe and tested the effect of these NPs on *Acanthamoeba triangularis* stages. KRe-loaded PEG-*b*-PCL, KRe-loaded niosome, and KRe-loaded PEG-*b*-PCL plus niosome were synthesized and characterized regarding particle size and charge, yield, encapsulation efficiency (EE), and drug loading content (DLC). The effect of these KRe-loaded NPs on trophozoite and cystic forms of *A. triangularis* was assessed through assays of minimal inhibitory concentration (MIC), using trypan blue exclusion to determine the viability. The effect of KRe-loaded NPs was also determined on *A. triangularis* trophozoite for 24–72 h. Additionally, the anti-adhesion activity of the KRe-loaded niosome on trophozoites was also performed on a 96-well plate. Cytotoxicity activity of KRe-loaded NPs was assessed on VERO and HaCaT cells using MTT assay.

Results. KRe-loaded niosome demonstrated a higher yielded (87.93 ± 6.03%) at 286 nm UV-Vis detection and exhibited a larger size (199.3 ± 29.98 nm) and DLC (19.63 ± 1.84%) compared to KRe-loaded PEG-*b*-PCL (45.2 ± 10.07 nm and 2.15 ± 0.25%). The EE (%) of KRe-loaded niosome was 63.67 ± 4.04, which was significantly lower than that of the combination of PEG-*b*-PCL and niosome (79.67 ± 2.08). However, the particle charge of these NPs was similar (−28.2 ± 3.68 mV and −28.5 ± 4.88, respectively). Additionally, KRe-loaded niosome and KRe-loaded PEG-*b*-PCL plus niosome exhibited a lower MIC at 24 h (0.25 mg/mL), inhibiting 90–100% of *Acanthamoeba* trophozoites which lasted 72 h. KRe-loaded niosome affected adherence by around 40–60% at 0.125–0.25 mg/mL and removed *Acanthamoeba* adhesion on the surface by about 90% at 0.5 mg/mL. Cell viability of VERO and HaCaT cells treated with 0.125 mg/mL of KRe-loaded niosome and KRe-loaded PEG-*b*-PCL plus niosome exceeded 80%.

Conclusion. Indeed, niosome and niosome plus PEG-*b*-PCL were suitable nanocarrier-loaded KRe, and they had a greater nanoparticle property to test with high activities against *A. triangularis* on the reduction of adherence ability and demonstration of its low toxicity to VERO and HaCaT cells.

Subjects Microbiology, Parasitology, Drugs and Devices, Infectious Diseases, Ophthalmology

Keywords *Acanthamoeba*, Phytoniosome, Niosome, *Knema retusa*, Nanoparticles, Drug delivery system, Protozoa, Parasite

INTRODUCTION

Acanthamoeba spp., waterborne protozoan parasites, are ubiquitous free-living amoebae found in environments such as water and soil (*Marciano-Cabral & Cabral, 2003*). This organism has two primary forms: the trophozoite, which is an invasive stage; and the cyst, which is a highly resistant stage that can endure very harsh conditions (*Marciano-Cabral & Cabral, 2003*). Although, *Acanthamoeba* infections are not highly prevalent, they remain a serious public health concern (*Marciano-Cabral & Cabral, 2003*), predominantly affecting chronically ill individuals, yielding over 90% mortality (*Kot, Łanocha-Arendarczyk &*

Kosik-Bogacka, 2021). The protozoa are causative agents of amebic keratitis (AK) and granulomatous amebic encephalitis (Marciano-Cabral & Cabral, 2003).

Treating AK is prolonged and demanding, although trophozoites, and immature cysts are substantially more responsive to multiple therapies than mature cysts (Chen et al., 2024). These facts underscore the pressing need for effective treatments against this parasitic pathogen (Chen et al., 2024). The treatment of this neglected pathogen is hampered by two major challenges: adverse effects and drug resistance (Sharma et al., 2020; Fanselow et al., 2021; Chen et al., 2024). Current therapy involves polyhexamethylene biguanide (PHMB; 0.02%–0.08%) and chlorhexidine (CHX; 0.02%), both of which can damage the cornea and cause corneal epitheliopathy (Shing et al., 2021). Miltefosine (MLF), an oral treatment for amoebas and leishmaniasis, has shown efficacy against *Acanthamoeba* (Schuster, Guglielmo & Visvesvara, 2006) with clinical success (Avdagic et al., 2021; Thulasi et al., 2021), however, resistance and toxicity are common (Matoba, Weikert & Kim, 2021; Thulasi et al., 2021). *Acanthamoeba* complicates treatment by surviving harsh conditions through dormancy, rather than genetic resistance. Consequently, current treatment regimens often exhibit limitations, highlighting the urgent need to identify safe and effective therapeutic agents against *Acanthamoeba* spp., while optimizing treatment and minimizing adverse effects.

Knema retusa (King) Warb. belongs to the Myristicaceae family and is a native plant in Peninsula Malaysia (Perak: Gunung Bubu) (Kew Royal Botanical Garden, 2023). This tree grows in wet tropical biome (Kew Royal Botanical Garden, 2023). The study showed that *Knema* genus and its active principles possessed a broad range of biological activities including antibacterial, anti-inflammatory, cytotoxicity, and acetylcholinesterase inhibitory activities (Salleh & Ahmad, 2017; Hop & Son, 2023). Recently, chloroform extracts of KRe woods possessed antibacterial activity in mastitis cows (Chuprom et al., 2023). Additionally, the antiparasitic activity on nematode was tested by the KRe plant extracts, which demonstrated a strong effect (Alen et al., 2000). Further studies of KRe on pharmacological activities and mechanisms are urgently suggested (Hop & Son, 2023). The increasing amount of data supports the application and exploitation of new drug development (Salleh & Ahmad, 2017).

Niosomes are non-ionic surfactant-based vesicles generated by the self-assembly of non-ionic surfactants in aqueous environments (Kazi et al., 2010). They are commonly used in the cosmetics industry and as drug carriers, including a potential role in targeted drug delivery systems in the future (Kazi et al., 2010). Niosomes offer several advantages over liposomes, including lower variability in purity, greater stability, and improved surfactant availability (Kazi et al., 2010). The non-ionic nature of the niosome also makes them safer regarding genotoxicity and provides structural flexibility. Furthermore, niosomes are low cost and more suitable for industrial manufacture than liposomes, as they do not need special procedures for preparation or storage (Kazi et al., 2010). Phytoniosome, or herbal extracts loaded with niosomes, have now been employed in the studies investigating biological activities such as antimicrobial, anticancer, and anti-*Acanthamoeba* activity (Al-Enazi et al., 2023; Sangkana et al., 2024).

Polymeric micelles (PMs) are formed by the self-assembly of amphiphilic block copolymers through solvophilic/solvophobic interactions (He et al., 2020). The core–shell

morphologies of PMs nanostructures create distinct domains varying with diverse chemical properties. As a result, PMs serve as essential pharmacological delivery vehicles for poorly water-soluble compounds (*Kwon, 2003*). PMs solubilize poorly soluble pharmaceuticals, provide controlled release, enhance stability under physiological conditions, and offer straightforward methods for drug release. Several studies have shown that PEG-*b*-PCL exhibits superior properties compared to other block copolymers due to the high hydrophobicity of PCL (*Theerasilp & Nasongkla, 2013*; *Eawsakul et al., 2017*; *Nasongkla et al., 2021*). Consequently, it can accommodate more hydrophobic substances compared to other polymers.

In this study, we formulated KRe loading-NPs including niosome, PEG-*b*-PCL PMs, and a combination of niosome and PEG-*b*-PCL. We also assessed the anti-*Acanthamoeba*, anti-adherent, and cytotoxicity activities of the KRe-loaded PEG-*b*-PCL, niosome, and their combination.

MATERIALS & METHODS

Preparation of plant extract

Plant material and extraction

The identity of *Knema retusa* was confirmed using a method reported by *Chuprom et al. (2023)*. Briefly, heartwood from mature trees in Manong and Kuala Kangsar, Perak, Malaysia, was collected. The wood was air-dried for two weeks, finely ground, and soaked in chloroform (1:5, w/v) at room temperature (RT) for three days. The extract was then filtered, concentrated under reduced pressure at 40 °C, air-dried, and prepared as a 100 mg/mL stock solution in dimethyl sulfoxide (DMSO), which was stored at −20 °C until use.

Preparation of KRe -loaded nanoparticles

Synthesis and characterization of PEG-b-PCL

The synthesis of PEG-*b*-PCL required ring-opening polymerization (*Eawsakul et al., 2017*). Initially, the moistened MeO–PEG–OH (2 g, 0.4 mmol) was dehydrated by applying heat at 65 °C and followed by vacuum. The ring-opening polymerization of ε-caprolactone with a molecular weight of 5 kDa was conducted in a reaction flask to synthesize PCL segment. Then, under an argon atmosphere, anhydrous toluene was introduced to the MeO-PEG-OH mixture. Finally, $Sn(Oct)_2$ catalyst was added. The entire procedure was conducted below 140 °C. Upon completion of the reaction, the mixture was cooled to RT. The PEG-*b*-PCL was refined by dissolving it in acetone and allowing it to precipitate in cold diethyl ether. After centrifugation, the PEG-*b*-PCL block copolymer was separated and lyophilized using a freeze-drying process. This work used PEG-*b*-PCL with Mn = 9.8 kDa, which was analyzed by nuclear magnetic resonance (^{1}H-NMR). The ^{1}H-NMR spectra (Bruker, MA, USA) were recorded on a Bruker AVANCE NEO 500 MHz spectrometer by dissolving 600 μL $CDCl_3$.

Preparation of KRe-loaded nanoparticles

KRe (drug) was incorporated three different types of nanoparticles (NPs): PEG-*b*-PCL block copolymer, niosome, and a mixture of PEG-*b*-PCL and niosome NPs. Following

prior studies, (1) drug loading into the PEG-*b*-PCL block copolymer was achieved through solvent evaporation (*Nasongkla et al., 2021*). During the preparation process, the initial KRe-to-PEG-*b*-PCL ratio was 1:9, and the manufacture of KRe-loaded niosomes was identical followed the same procedure as that the PEG-*b*-PCL block copolymer. (2) For drug loaded in the niosome, the ratio of span 60 to cholesterol was 12.9:7.7 (*Miatmoko et al., 2021*). Then, 10 mg of KRe was added as an anti-*Acanthamoeba* model to the solution. (3) The mixture of drug-loaded PEG-*b*-PCL block copolymers and niosome was fabricated by solvent evaporation. The proportions of the components were as follows: PEG-*b*-PCL, span 60, cholesterol, and drug were prepared by dissolving in chloroform in the ratio of 90:12.9:7.7:10. The chloroform in these samples was evaporated using a magnetic stirrer overnight after being added dropwise to 10 mL of water using a probe sonicator (Model CV.18; Sonics, Newtown, CT, USA) and sonicated for two minutes at an amplitude of 80%. For the subsequent experiments, samples were refrigerated at 4 °C.

Particle size and charge

After KRe was loaded into three distinct nanoparticle (NP) types, the particle size and surface charges were analyzed using the dynamic light scattering (DLS) and a Malvern Zeta Sizer (Malvern Instruments, Worcestershire, UK) (*Eawsakul et al., 2017*; *Nasongkla et al., 2021*; *Ongtanasup et al., 2024*). Samples were prepared by first performing a 20-fold dilution in water, followed by three successive measurements per sample to reduce the measurement error. The zeta potential was calculated utilizing the Smoluchowski approximation. DLS measurements were conducted over 20 separate 10s runs, with a 10s equilibration interval between each run. Each sample was examined at 25 °C, and a laser wavelength of 633 nm, with a scattering angle of 173°, a medium viscosity of 0.8872 cP, and an index of refraction of 1.33.

Determination of yield, encapsulation efficiency, and drug loading content

NP yield, encapsulation efficiency (EE), and drug-loaded content (DLC) were measured (*Eawsakul et al., 2017*; *Nasongkla et al., 2021*). First, NP aggregation was eliminated by centrifugation at 5,000 rpm for 15 min at 4 °C. Next, the free KRe in NPs was identified using a centrifugal filter with a 50 kDa molecular cut-off. To obtain the powder, the solution from the top (KRe-loaded NP) and bottom (free KRe) centrifugal filters were freeze-dried. To verify the encapsulated drug, the powder was weighed, the yield was determined (Eq. (1)), and it was dissolved in a 20:80 combination of ethanol (EtOH) and phosphate buffered saline (PBS). The KRe concentration in the extracted solution was determined, and then the KRe loading content and EE were calculated (Eqs. (2) and (3)) as follows:

$$\%Yield = \frac{Weight\ of\ nanoparticle}{Theoretical\ total\ amound\ of\ nanoparticle} * 100 \quad (1)$$

$$\%DLC = \frac{Amount\ of\ encapuslated\ KRe\ in\ nanoparticle}{Weight\ of\ nanoparticle} * 100 \quad (2)$$

$$\%EE = \frac{Amount\ of\ encapsulated\ KRe\ in\ nanoparticle}{Initial\ amound\ of\ KRe} * 100 \quad (3)$$

Acanthamoeba culture and anti-*Acanthamoeba* activity

Based on the biosafety guidelines for scientific research at Walailak University, Thailand (Ref. no. WU-IBC-66-020), all experiments were carried out accordingly. *Acanthamoeba triangularis* WU19001, a strain from the recreational reservoir at Walailak University, Nakhon Si Thammarat, Thailand (*Mitsuwan et al., 2020*), and *A. castellanii* ATCC30010, *A. castellanii* ATCC50739, and *A. polyphaga* ATCC30461, were used in this study. Trophozoites of the *Acanthamoeba* strains were grown in Peptone-Yeast-Glucose (PYG) medium (20 g proteose peptone, 2 g yeast extract, 0.98 g $MgSO_4 \cdot 7H_2O$, 0.35 g $Na_2HPO_4 \cdot 7H_2O$, 0.34 g KH_2PO_4, 0.02 g $(NH4)_2Fe(SO_4)_2 \cdot 6H_2O$, 18 g glucose and 1,000 mL distilled water (DW)] and incubated at RT for 3 days. The mature cyst forms of *Acanthamoeba* species was cultured in Neff's medium (containing g/L; 7.45 g KCl, 2.44 g (2-amino-2-methyl-1,3-propanediol), 0.09 g $NaHCO_3$, 1.97 g $MgSO_4.7H_2O$, 0.06 g $CaCl_2.2H_2O$, and DW) at RT for at least 7 days.

To determine the effect of different types of NPs containing KRe (KRe-loaded PEG-*b*-PCL, niosome and PEG-*b*-PCL plus niosome) on *Acanthamoeba* viability, the determination of the minimal inhibitory concentration (MIC) was evaluated using a trypan blue exclusion assay (*Mitsuwan et al., 2020*; *Mitsuwan et al., 2021*). Briefly, 100 μL of the KRe NPs serially diluted in two-folded to give a final concentration range (1–0.0625 mg/mL) was added to a 96-well plate. Then, 100 μL of trophozoites (2×10^5 cells/mL) was seeded in each well. Further, 1% DMSO and CHX (0.001–0.128 mg/mL) were used as negative and positive controls. The plates were incubated at RT for 24 h. Then, the MIC values were evaluated. The MIC value was obtained from the enumeration of trophozoites and cysts viability using the trypan blue exclusion method. Viability was investigated under the inverted microscope (Nikon ECLIPSE TE2000-S; Nikon, Tokyo, Japan) based on the principle that the dye can cross the membrane of dead cells with a blue color but not the intact membrane of viable cells with a colorless appearance. For counting, 50 μL of trophozoites and cysts containing the diluted KRe-loaded PEG-*b*-PCL, niosome, and PEG-*b*-PCL plus niosome suspension were placed on a new well plate, and 50 μL of 0.2% trypan blue dye was then added. It was incubated at RT for 5 min. The cell suspensions mixed with trypan blue dye (10 μL) were placed on a hemocytometer (Boeco, Hamburg, Germany). Cell viability was then enumerated under inverted microscopy. MIC is defined as the lowest concentration of the tested NPs that inhibits greater than 90% of *Acanthamoeba* viability. The relative percentage of trophozoites and cysts viability was defined as Eq.(4).

$$\text{Relative } \textit{Acanthamoeba} \text{ Inhibition} = \left[\frac{(\textit{Acanthamoeba} \text{ viability tested by KRe} - \text{Loaded nanoparticles})}{\textit{Acanthamoeba} \text{ viability tested by control}}\right] * 100 \quad (4)$$

To assess *Acanthamoeba*'s ability to endure harsh conditions and treatments, and to determine whether it temporarily halts growth, *A. triangularis* trophozoites (2×10^5 cells/mL) were incubated in NP solutions with 1/2 MIC (0.125 mg/mL) and

Table 1 Characterization of different nanoparticles containing *Knema retusa* extract.

Characteristics	KRe-loaded PEG-*b*-PCL	KRe-loaded niosome	KRe-loaded PEG-*b*-PCL and niosome
Drug loading content (% DLC)	2.15 ± 0.25^{a}	19.63 ± 1.84^{b}	7.42 ± 0.36^{c}
Encapsulation efficiency (% EE)	18.00 ± 2.65^{a}	63.67 ± 4.04^{b}	79.67 ± 2.08^{c}
Yield (%)	83.67 ± 3.13^{ns}	87.93 ± 6.03^{ns}	84.59 ± 2.47^{ns}
Size (nm)	45.2 ± 10.07	199.3 ± 29.98	167.1 ± 25.57
PdI	0.050	0.023	0.023
Charge (mV)	-9.29 ± 3.68^{a}	-28.2 ± 3.72^{ab}	-28.5 ± 4.88^{ac}

Notes.

%DLC, %EE, and % Yield data represent mean ± SD, Size and charge represent mean ± width; Different letters (row) denote significant difference using One-way ANOVA analysis.

ns, not significant; KRe, *Knema retusa* extract; PEG-*b*-PCL, Poly(ethylene glycol)-block-poly (ε- caprolactone); PdI, Polydispersity index.

1 MIC (0.25 mg/mL). The viability of *Acanthamoeba* was evaluated at 24, 48, and 72 h using trypan blue staining, as previously described (*Mitsuwan et al., 2020*).

Anti-adhesion activity

The KRe-loaded niosome exhibited superior nanoparticle properties showing higher percentages of yield, DLC and EE than the other formulation. Its activity demonstrated significant potential on *A. triangularis* trophozoites (Tables 1–2). To further investigate the effect of KRe-loaded niosome on anti-adhesion activity of *A. triangularis* trophozoites, an experiment was conducted on a 96-well polystyrene plate (0.33 cm^2 of culture area, 0.075–0.2 mL of proposed working volume, VWR International, Missouri, USA) (*Sama-Ae et al., 2022*). Briefly, trophozoites (4×10^5/mL) were cultured in PYG supplemented with KRe-loaded niosome at 0.0625 mg/mL (1/4 MIC) and 0.125 mg/mL (1/2MIC) to determine the effect of the NPs on adhesion activity. To study the effect of the NPs on adhesive removal, 100 µL of trophozoites (4×10^5 cells/mL) were inoculated in PYG on a 96-well plate and incubated at RT for 48 h. KRe-loaded niosome then treated the trophozoites at concentration of 0.25 mg/mL (1MIC) and 0.50 mg/mL (2MIC) for 24 h. CHX (2MIC; 0.016 mg/mL, 1MIC; 0.008 mg/mL, 1/2MIC; 0.004 mg/mL, and 1/4MIC; 0.002 mg/mL) and 1% DMSO were used as positive and negative controls, respectively. Non-adhesive cells were eliminated by removing the old medium, which was washed twice with Page's Saline (PAS) solution. To detect the adhesion of trophozoites on the 96-well plate, samples were stained with 0.1% crystal violet for 30 min, subsequently washed twice with sterile DW, and air dried overnight at RT. Then, 200 µL of DMSO were added to dissolve the stained cells. Plates were measured at an optical density (OD) of 570 nm. The activity of KRe-loaded niosome on *A. triangularis* adhesion was calculated as a relative percentage of the adhesion as follows:

$$Adhesion(\%) = \frac{Mean\ A570\ nm\ of\ \ treated\ well}{Mean\ A570\ nm\ of\ \ control\ well} * 100 \quad (5)$$

Cytotoxicity assay

The cell viability assay was performed, as previously described (*Chimplee et al., 2022*; *Sama-Ae et al., 2022*). The cytotoxicity of KRe-unloaded and KRe-loaded NPs was assessed

Table 2 Minimal inhibitory concentration and half maximal inhibitory concentration of different nanoparticles loading *Knema retusa* extract on *Acanthamoeba* species and mammalian cell lines for 24 h.

Nanoparticles	MIC (mg/mL)								IC_{50} (mg/mL)	
	Acanthamoeba (Trophozoites)				*Acanthamoeba* (Cysts)				Vero	HaCaT
	AT	AC3	AC5	AP	AT	AC3	AC5	AP		
KRe-loaded PEG-*b*-PCL	>1	>1	>1	>1	>1	>1	>1	>1	0.585	0.587
KRe-loaded niosome	0.25	>1	1	>1	>1	>1	>1	>1	0.311	0.317
KRe-loaded PEG-*b*-PCL and niosome	0.25	>1	1	>1	>1	>1	>1	>1	0.210	0.171
CHX	0.008	0.008	0.016	0.016	0.064	>0.0128	0.032	>0.0128	nd	nd

Notes.

MIC, (Minimal inhibitory concentration) means 90% *Acanthamoeba* inhibition; IC_{50}, maximum inhibitory concentration at 50% cell inhibition; CHX, Chlorhexidine; AT, *A.triangularis* WU19001; AC3, *A.castellanii* ATCC30010; AC5, *A.castellanii* ATCC50739; AP, *A.polyphaga* ATCC30461; nd, not detected; KRe, *Knema retusa* extract; PEG-*b*-PCL, Poly(ethylene glycol)-block-poly (ε-caprolactone).

using Vero cells (ECACC 84113001, RRID: CVCL 0059, Salisbury, UK) provided by Assoc. Prof. Dr. Chuchard Punsawad, School of Medicine, Walailak University. Human epidermal keratinocyte (HaCaT) cells (Cytion cat no. 300493; DKFZ; CLS Cell Lines Service, Heidelberg, Germany) were also tested, courtesy of Assoc. Prof. Dr. Warangkana Chunglok and Dr. Nichaporn Wongsirojkul, School of Allied Health Sciences, Walailak University. Both cell lines were cultured in Dulbecco's Modified Eagle's medium (DMEM; Merck KGaA, Darmstadt, Germany) supplemented with 10% fetal bovine serum (FBS; Sigma Aldrich, St. Louis, MO, USA) and 1% penicillin-streptomycin, and were incubated at 37 °C with 5% CO_2. Once the cells reached 90% confluence, they were detached with trypsin-EDTA and incubated for additional 5 mins. Vero cells (1.5×10^4 cell/mL) and HaCaT cells (5×10^3 cell/mL) were seeded in 96-well plates and allowed to attach for 24 h before the addition of KRe-unloaded and KRe-loaded NPs. After another 24 h, cytotoxicity was assessed using an MTT assay, with absorbance measured at 570 nm and 650 nm. The survival percentage was calculated using the following equation:

$$Survival(\%) = \frac{ABt\ 570\ nm - ABt\ 650\ nm}{ABu\ 570\ nm - ABu\ 650\ nm} * 100 \quad (6)$$

ABt and ABu denote the absorbance values of treated and untreated cells, respectively.

IC_{50} values were then calculated from a fitted response curve plotted using the cell viability (%) and concentration based on a non-linear regression (curve fit) model. Data are presented as the mean ± SD from three independent replicates.

Statistical analysis

All experiments were performed in triplicates across three dependent experiments. Data was recorded and analyzed using GraphPad Prism 10 (GraphPad Software, San Diego, CA, USA). Additionally, two-way ANOVA was also used to analyze the statistical significance of adhesion and removal ability. Results are presented as mean ± SD, with $p < 0.05$ considered a statistically significant difference.

RESULTS

Characterization of PEG-*b*-PCL

To describe the structure and molecular weight of the copolymer (PEG-*b*-PCL), ^{1}H NMR spectra (in $CDCl_3$) were acquired, as shown in Fig. 1A. The solvent peak of $CDCl_3$ was detected at 7.26 ppm in the ^{1}H NMR spectrum. The chemical shifts and peak assignments are as follows in Fig. 1A: the peaks at 1.3 ppm (2H of middle epsilon-CL), 1.6 ppm (4H of middle epsilon-CL), 2.3 ppm (2H of CO-CH_2), and 4.1 ppm (2H of CH_2-OH) were attributed to the PCL part, whereas the peaks at 3.38 ppm (3H of CH_3-O) and 3.6 ppm (4H of O-CH_2-CH_2-) were assigned to the PEG part.

Characterization of KRe-loaded nanoparticles

The three distinct types of nanocarriers were loaded with KRe using a solvent evaporation method. The KRe and its associated nanocarrier were dissolved in chloroform and then added to deionized water under continuous sonication. The non-capsulated KRe was removed using a centrifugal filter with a 50 kDa cut-off. Lyophilized formulations were dissolved in a mixture solution of EtOH and PBS and analyzed using an ultraviolet–visible (UV-vis) spectrophotometer at a wavelength of 286 nm (Figs. 1B–1C) to determine yield, EE, and DLC as indicated in Table 1.

Considering the size of NPs in Table 1 and Figs. 1D, 1E, it has been observed that KRe-loaded niosomes can contain a large amount of KRe but have a larger particle size (199.3 ± 29.98 nm). In comparison, KRe loaded in PEG-*b*-PCL has a smaller particle size (approximately 45 ± 10.07 nm) but contain less KRe overall. The charge of the smaller PEG-*b*-PCL was −9.29 ± 3.68 mV, while the charge of the niosome with the larger particle size was −28.2 ± 3.68 mV. For the combined nanocarriers, the experiment showed that the KRe loading into both niosome and PEG-*b*-PCL NPs was suitable, with KRe loaded combined NPs exhibiting the highest negative charge at −28.5 ± 4.88 mV.

Effect of KRe -loaded nanoparticles on *Acanthamoeba*

All the tested KRe-loaded NPs exhibited a weak inhibitory effect (<90%) on cysts regardless of the *Acanthamoeba* species, indicating that the MIC values for these resistant forms were higher than 1 mg/mL. Table 2 shows the MIC values for *Acanthamoeba* trophozoites and cysts inhibition tested with different types of KRe-loaded PEG-*b*-PCL, niosome, and PEG-*b*-PCL plus niosome NPs against *A. triangularis* and other species. MIC value indicating greater than 90% inhibition of *Acanthamoeba* were found at 0.25 and 1 mg/mL from both KRe-loaded niosome, and KRe-loaded PEG-*b*-PCL plus niosome nanocarriers for 24 h of treatment on *A. triangularis* and *A. castellanii* ATCC50739 (Table 2). In contrast, the MIC of the tested KRe-loaded PEG-*b*-PCL NP was higher than 1 mg/mL against all *Acanthamoeba* species (Table 2). To determine the efficacy of the three NPs in inhibiting the re-growth of *Acanthamoeba* trophozoites, the NPs were tested at various concentrations (MIC; 0.25 mg/mL and 1/2MIC; 0.125 mg/mL) and time intervals (24, 48, and 72 h) depending on the selected species (Table 3). At MIC 0.25 mg/mL, KRe-loaded niosome provided the greatest inhibition of *Acanthamoeba* (averaged ± SD (%), 100.00 ± 0.00, 97.75 ± 1.74, 97.35 ± 0.00), followed by KRe-loaded PEG-*b*-PCL plus niosome

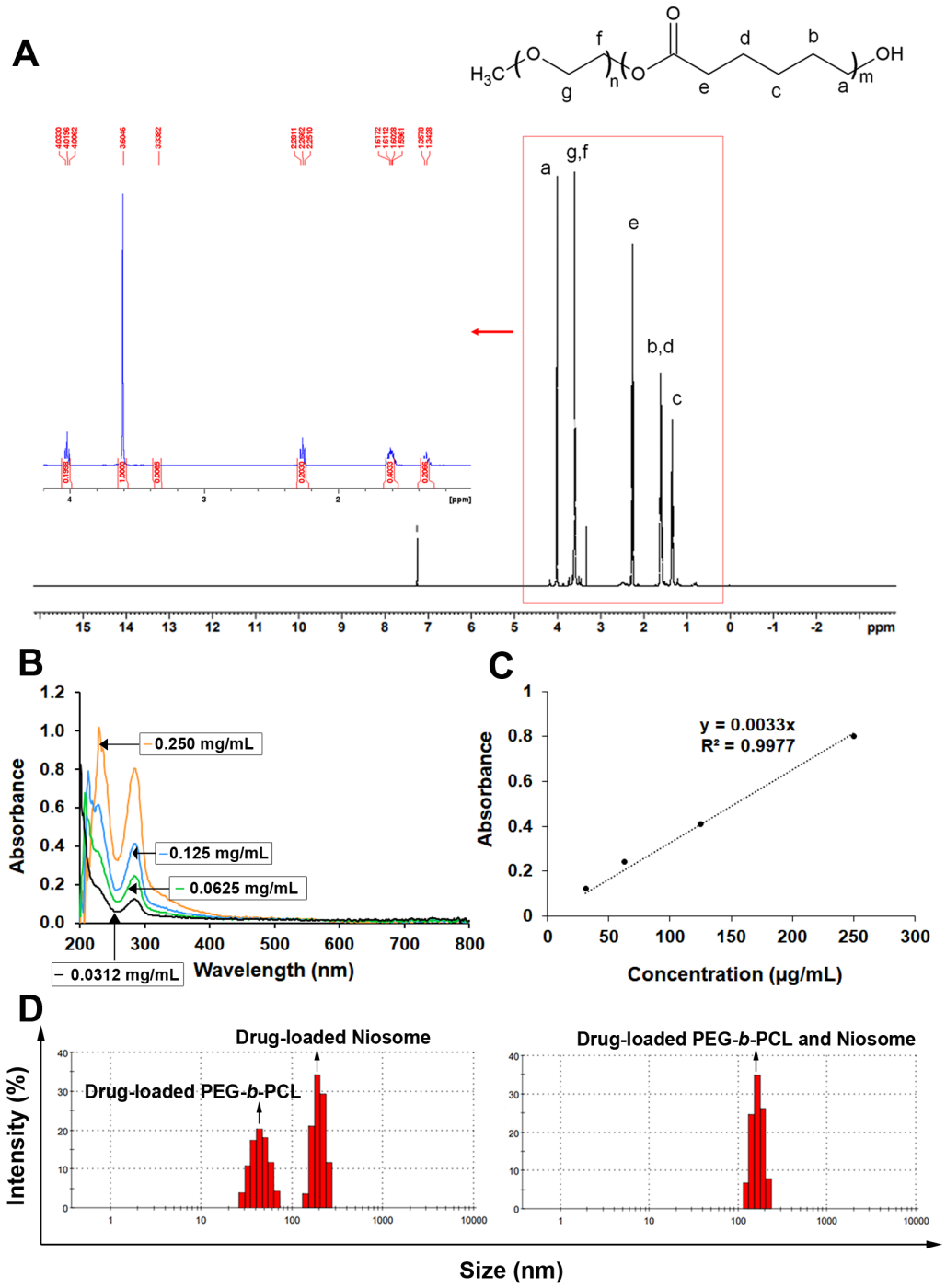

Figure 1 Characteristics of various synthesized polymers with nanoparticles containing KRe. (A) ^{1}H NMR spectrum of PEG-*b*-PCL (B) UV spectrum of KRe; the UV-vis absorption of KRe at different concentrations; 0.250 mg/mL (orange), 0.125 mg/mL (sky blue), 0.0625 mg/mL (bluish green), and 0.0312 µg/mL (black). (C) Standard curve of KRe. (D) Morphology and histogram of KRe loaded-nanoparticles; PEG-*b*-PCL, niosome, and PEG-*b*-PCL plus niosome analyzed by dynamic light scattering (DLS) technique.

Full-size DOI: 10.7717/peerj.18452/fig-1

Table 3 ***Anti-Acanthamoeba*** **activity of different nanoparticles loading** ***Knema retusa*** **extract on** ***A. triangularis*** **WU 19001.**

Time (h)	Concentration (mg/mL)	*Acanthamoeba* inhibition (%, mean ± SD)		
		KRe-loaded PEG-*b*-PCL	KRe-loaded niosome	KRe-loaded PEG-*b*-PCL and niosome
24	0.250	17.95 ± 7.16^{a}	100.00 ± 0.00^{b}	87.18 ± 1.99^{c}
	0.125	25.64 ± 3.97^{ns}	7.69 ± 5.25^{a}	32.05 ± 7.16^{ab}
48	0.250	38.20 ± 8.53^{a}	$97.75 \pm 1.74^{ab,ns}$	$86.52 \pm 5.22^{ac,ns}$
	0.125	26.97 ± 5.15^{ns}	48.31 ± 4.61^{a}	38.20 ± 4.61^{b}
72	0.250	38.05 ± 1.37^{a}	$97.35 \pm 0.00^{ab,ns}$	$87.61 \pm 3.63^{ac,ns}$
	0.125	30.97 ± 4.11^{a}	49.56 ± 2.37^{ns}	42.48 ± 4.94^{ab}

Notes.

Different letters (row) denote significant difference using One-way ANOVA analysis.

ns, not significant; KRe, *Knema retusa* extract; PEG-*b*-PCL, Poly(ethylene glycol)-block-poly (ε- caprolactone).

(averaged ± SD (%), 87.18 ± 1.99, 86.52 ± 5.22, and 87.61 ± 3.63), and KRe-loaded PEG-*b*-PCL (averaged ± SD (%), 17.95 ± 7.16, 38.20 ± 8.53, and 38.05 ± 1.37) at 24, 48, 72 h treatment, respectively (Table 3). Additionally, an increase in the percentage of *Acanthamoeba* inhibition was observed at 1/2MIC (0.125 mg/mL) after treatment with KRe-loaded niosome (averaged ± SD (%), 7.69 ± 5.25, 48.31 ± 4.61, and 49.56 ± 2.37), KRe-loaded PEG-*b*-PCL plus niosome (averaged ± SD (%), 32.05 ± 7.16, 38.20 ± 4.61, and 42.48 ± 4.94), and KRe-loaded PEG-*b*-PCL (averaged ± SD (%), 25.64 ± 3.97, 26.97 ± 5.15, and 30.97 ± 4.11) for 24 h, 48 h and 72 h (Table 3). The results suggested that KRe-loaded niosome at MIC (0.25 mg/mL) is an effective concentration for suppressing trophozoites when treated for a longer duration, compared to treated *Acanthamoeba* at 1/2MIC (0.125 mg/mL). Additionally, all of the tested KRe-loaded NPs demonstrated a weak inhibitory effect (<90% *Acanthamoeba* inhibition) on all of the tested cystic forms of *Acanthamoeba* species at 1 mg/mL. The results indicate that MIC values for those tested NPs against *Acanthamoeba* cysts were greater than 1 mg/mL (Table 2).

Effect of KRe -loaded niosome on trophozoites adhesion on plastic surface

This study found that the KRe-loaded niosome NP (1MIC, 0.25 mg/mL) exhibited the strongest and most consistent suppression on *A. triangularis* viability, it was subsequently investigated whether this treatment affected the adhesive ability of *Acanthamoeba* trophozoites. The results revealed that treating KRe-loaded niosome with *A. triangularis* for 24 h significantly reduced the adhesion of trophozoites to 40% at 1/2MIC (0.125 mg/mL) and 60% at 1/4MIC (0.625 mg/mL), compared to a positive control (about 70% at CHX 1/2MIC; 0.004 mg/mL and 80% at CHX 1/4MIC; 0.002 mg/mL) and negative control (about 100% at 1% DMSO), as shown in Fig. 2A.

Additionally, it was found that treating of KRe-loaded niosome for 24 h could significantly decrease 48 h-adhesion of trophozoites to the surface, with about 80% removal at 1MIC (0.25 mg/mL) and 90% removal at 2MIC (0.5 mg/mL), compared to the

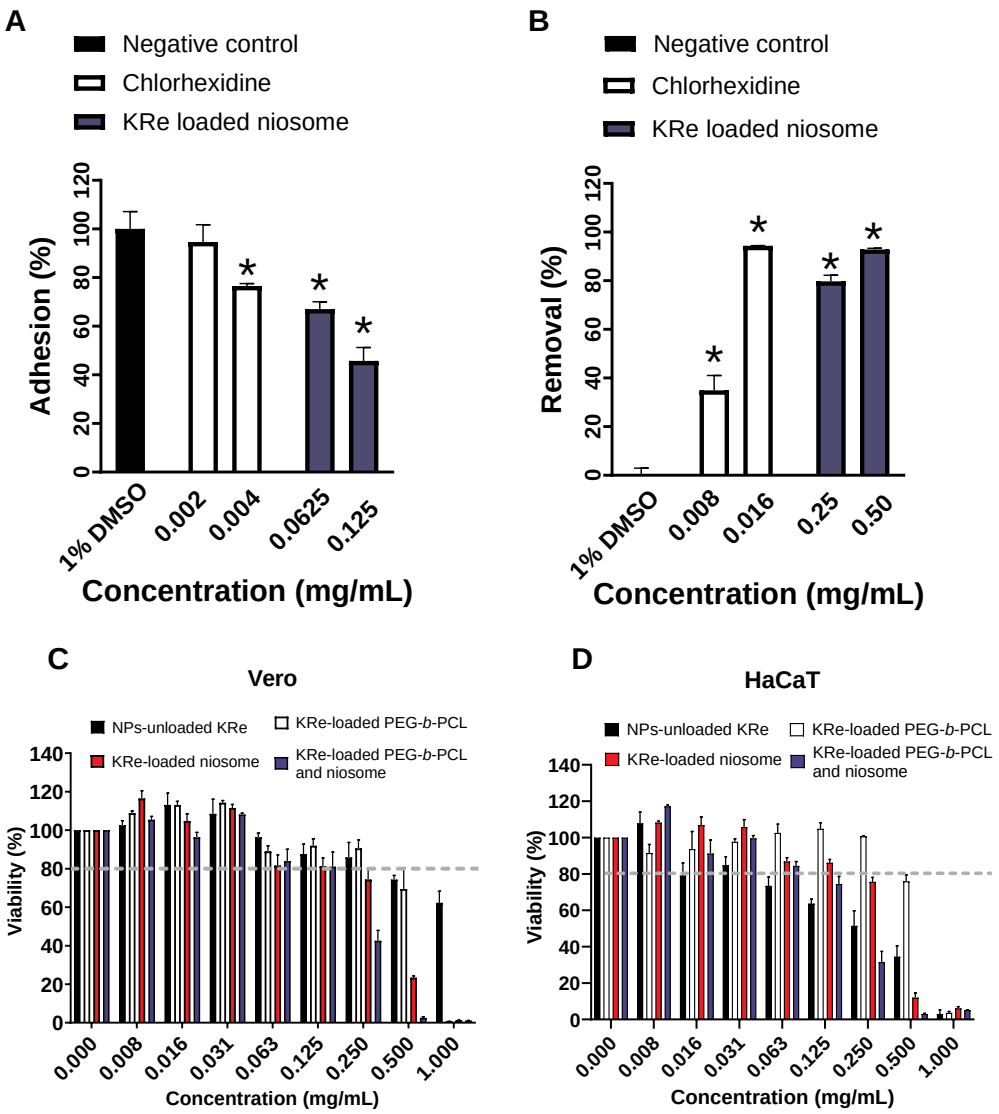

Figure 2 Effects of KRe-loaded niosome on the adhesion and removal of *Acanthamoeba triangularis* trophozoites on the plastic surface and its cytotoxicity on mammalian cell lines. Effects of KRe-loaded niosome on the adhesion (A) and removal (B) of *Acanthamoeba triangularis* trophozoites on the plastic surface. KRe-loaded niosome (2MIC; 0.5 mg/mL, 1MIC; 0.25 mg/mL, 1/2MIC; 0.125, 1/4MIC; 0.0625 mg/mL). Chlorhexidine (2MIC; 0.016 mg/mL, 1MIC; 0.008 mg/mL, 1/2MIC; 0.004 mg/mL, and 1/4MIC; 0.002 mg/mL) and 1% DMSO were used as positive and negative controls, respectively. The relative percentage of adhesion and removal of the treated cells compared with the negative control were assessed (*significant difference; $p < 0.05$). (C–D) Cytotoxicity of KRe-unloaded and KRe-loaded nanoparticles on Vero (C) and HaCaT (D) cells. NPs, nanoparticles.

Full-size DOI: 10.7717/peerj.18452/fig-2

activity (% removal) from CHX (40% at 1MIC; 0.008 mg/mL) and 1% DMSO (about 1%) (Fig. 2B). The adhesive removal ability of the NPs treatments (40–90% removal) showed no significant difference, compared to CHX 1MIC; 0.008 mg/mL and 2MIC; 0.016 mg/mL (80–90% removal) (Fig. 2B).

In vitro cytotoxicity

The IC_{50} values (Table 2) for KRe-unloaded NP (KRe-free compound) were 1.238 mg/mL in normal kidney Vero cells, while the IC_{50} of KRe-loaded PEG-*b*-PCL, KRe-loaded niosome, and KRe-loaded PEG-*b*-PCL plus niosome were 0.585, 0.311, and 0.210 mg/mL, respectively. Additionally, the IC_{50} values for KRe-unloaded NP in keratinocyte HaCaT cells were 0.224 mg/mL with the IC_{50} values for KRe-loaded PEG-*b*-PCL, KRe-loaded niosome, and KRe-loaded PEG-*b*-PCL plus niosome being 0.587, 0.317, and 0.171 mg/mL, respectively. According to ISO 10993-5, when cell viability exceeds 80%, the compound is considered non-cytotoxic, whereas a cell viability range between 60–80% indicates weak cytotoxicity (*International Organization for Standardization, 2009*; *Chuprom et al., 2022*). Our results revealed that after 24 h of treatment with KRe-unloaded and KRe-loaded NPs, the number of viable Vero and HaCaT cells was reduced to below 80% at higher concentrations, ranging from 0.5–1 mg/mL (Figs. 2C–2D). It was noted that the survival rate of Vero and HaCaT cells was lower than 80% when treated with those NPs at lower concentrations of 0.008–0.25 mg/mL (Figs. 2C–2D). It was noted that in both Vero (Fig. 2C) and HaCaT cells (Fig. 2D), cell viability remains relatively high, above 80%, across all NP formulations (unloaded KRe, KRe-loaded PEG-*b*-PCL, KRe-loaded niosome, and KRe-loaded PEG-*b*-PCL with niosome) in the lower concentration range of 0.008 to 0.25 mg/mL. However, a slight downward trend as concentrations increases towards 0.25 mg/mL was observed in both Vero and HaCaT cells.

DISCUSSION

The major constituents of the KRe were studied for their water solubility properties using the Swiss-ADME tool (*Ongtanasup et al., 2022*). The study has recently reported that most compounds in the KRe were water-soluble, including benzenamine (5-methoxy-2-methyl aniline (8.98%), exo-2-hydroxy-9, 9-(ethylenedioxy)-1-carbethoxybicyclo [3.3.1] nonane (64.83%), and palmitic acid (5.27%) (*Chuprom et al., 2023*). Therefore, the noisome—a drug delivery system capable of containing water-soluble compounds—was more effective than polymeric micelles made from PEG-*b*-PCL for incorporating these KRe substances. Given the hydrophilic property of the KRe, it is more soluble in polar environments than in nonpolar ones, which the hydrophilic component of the niosome facilities. Niosomes also contribute to a broader hydrophilic domain (*Chen et al., 2019*), resulting in better encapsulation effectiveness. In contrast, the lowest encapsulation achieved with PEG-*b*-PCL is due to its less hydrophilic nature and its larger area of hydrophobic domains (*Brandt et al., 2019*; *Nasongkla et al., 2021*), resulting in a smaller free volume available for encapsulating the KRe. However, it was discovered that the KRe also contains molecules that are insoluble in water (*Chuprom et al., 2023*). As chloroform with higher vapor pressure evaporated during the encapsulation of KRe using the technique in this study, the KRe became less soluble, leading to the formation of nanocarriers. The KRe could then be loaded into the nanocarriers, resulting in an insoluble complex. The introduction of both types of nanocarriers for loading of KRe can enhance the drug loading efficiency because PEG-*b*-PCL effectively encapsulates water-insoluble compounds, while niosome can accommodate water-soluble compounds efficiently.

The data demonstrates that the inclusion of both nanocarriers for the loading of KRe increases the loading efficiency of KRe compared to loading with either PEG-*b*-PCL or niosome. In experiment involving the combined nanocarriers, nanocarriers, the size of KRe loaded into both niosome and PEG-*b*-PCL NPs was (167.1 ± 25.57 nm), which indicates that these are suitable nanocarriers. Addiotionally, the KRe loaded in mixed nanoparticles of niosomes and PEG-*b*-PCL exhibited the highest negative charge at −28.5 ± 4.88 mV; the higher the negative charge, contributes to greater prevention of precipitation due to charge repulsion. However, the charge of KRe-loaded niosome (−28.2 ± 3.72 mV) was not significantly different from that of KRe-loaded niosome plus PEG-*b*-PCL, and the excellent constituent assembly of the KRe-loaded niosome was also detected. The size of KRe-loaded niosomes was less stable at 199.3 ± 29.98 nm, which was larger than the KRe-loaded niosome plus PEG-*b*-PCL. The size of KRe-loaded niosome NP falls within the acceptable range of common types of niosome (large unilamellar vesicles, 100–3,000 nm), and the larger size of KRe-loaded niosome may be attributed to the increasing of KRe loading in the niosome particle (%DLC = 19.63 ± 1.84) (*Ge et al., 2019*).

In our study, it was assumed that both the KRe-loaded niosome and KRe-loaded niosome plus PEG-*b*-PCL supported the potential activity of *A. triangularis* and *A. castellanii* ATCC50739 trophozoites viability. The inhibitory effects of both nanocarriers demonstrated effective inhibition of *A. triangularis* trophozoites over a given treatment period and showed potential for suppressing adherent ability, as well as eliminating *A. triangularis* trophozoites adhesion on the plastic surface. The study suggests that niosome hold great potential as a drug delivery system against parasitic infections including *Acanthamoeba*, ocular keratitis caused by *Candida albican* and other infectious microbial activities (*Barani et al., 2023*; *Gugleva et al., 2023*; *Sangkana et al., 2024*). To support this, a previous study indicated that niosome-loaded natamycin improved treatment effectiveness and side effects after long-term treatment of keratitis caused by fungal infections (*El-Nabarawi et al., 2019*). Furthurmore, niosomal-PEG NPs co-loaded with metformin and silibinin proved to be an effective treatment for human lung cancer cells (*Salmani-Javan et al., 2023*). Unfortunately, the KRe-loaded NPs exhibited only waek lethality against the cyst form of *Acanthamoeba* spp., and possibly due to the double-walled structure strength of the cyst, which presents a crucial barrier for drugs targeting the amoeba residing within the shell (*Anwar, Khan & Siddiqui, 2018*).

The cytotoxicity of KRe-free and KRe-loaded NPs towards Vero and HaCaT cells was investigated using the MTT assay (Figs. 2C–2D and Table 2). According to *International Organization for Standardization (2009)*, the application of various nanocarriers of NPs showed no improvement in the safety of normal kidney Vero cells, as both KRe-free and KRe-loaded NPs exhibited slight toxicity, resulting in reduced cell viability, unlike KRe-co-loaded noisome and PEG-*b*-PCL, which showed about 40% viability. The safety of the tested nanocarriers was found to be better for skin keratinocyte HaCaT cells, which represent keratinocytes in corneal tissue compared to KRe-free NPs. HaCaT cells exhibited was more than 80% viability with KRe-loaded PEG-*b*-PCL and KRe-loaded niosome at 0.25 mg/mL, while KRe-loaded PEG-*b*-PCL and niosome demonstrated less than 40% viability, in contrast to KRe-free NPs, which showed approximately 50% viability.

Additionally, KRe-free shows weak cytotoxicity (60–80% cell survival) at concentration ranging from 0.625–0.125 mg/mL and strong toxicity (<60% survival) at 0.25 to 1 mg/mL. To minimize normal toxicity on both Vero and HaCaT cells, KRe-loaded niosome with KRe-loaded niosome and PEG-*b*-PCL should be administered at an optimized concentration of 0.125 mg/mL. Notably, KRe-loaded niosome was safer for normal HaCaT cells than KRe-free at a high concentration of 0.25 mg/mL. IC_{50} values of nanocarriers on Vero and HaCaT, ranged from 0.171–0.587 mg/mL (Table 2), indicating low toxicity. *González-Larraza et al. (2020)* reported the study evaluating cytotoxicity of nano-platinum on fibroblasts, which yielded a high IC_{50} at 0.160 ± 11.29 mg/mL, indicating its safety.

CONCLUSIONS

To our knowledge, niosome and niosome mixed PEG-*b*-PCL were suitable nanocarrier for loading KRe. They demonstrated the enhanced NP property for testing, exhibiting high activity against *Acanthamoeba*, particularly in reducing the viability of *A. triangularis* trophozoites, as well as facilitating the removal of *Acanthamoeba* adhesion from the surface. This promising medicinal plant warrants further investigations in the future.

ACKNOWLEDGEMENTS

The authors would like to thank Asst. Prof. Dr. Sirirat Surinkaew for her kind assistance in providing reagents for cell culture experiments.

ADDITIONAL INFORMATION AND DECLARATIONS

Funding

This work was supported by The Royal Patronage of Her Royal Highness Princess Maha Chakri Sirindhorn-Botanical Garden of Walailak University, Nakhon Si Thammarat, Thailand (Grant No. RSPG-WU-14/2567) and Project CICECO-Aveiro Institute of Materials, UIDB/50011/2020, UIDP/50011/2020 & LA/P/0006/2020, financed by national funds through the FCT/MEC (PIDDAC). The funders had no role in study design, data collection and analysis, decision to publish, or preparation of the manuscript.

Grant Disclosures

The following grant information was disclosed by the authors:
The Royal Patronage of Her Royal Highness Princess Maha Chakri Sirindhorn-Botanical Garden of Walailak University, Nakhon Si Thammarat, Thailand: RSPG-WU-14/2567.
Project CICECO-Aveiro Institute of Materials: UIDB/50011/2020, UIDP/50011/2020, LA/P/0006/2020.
FCT/MEC (PIDDAC).

Competing Interests

Sónia MR Oliveira is an Academic Editor for PeerJ.

Author Contributions

- Siriphorn Chimplee analyzed the data, prepared figures and/or tables, authored or reviewed drafts of the article, and approved the final draft.
- Watcharapong Mitsuwan conceived and designed the experiments, performed the experiments, analyzed the data, prepared figures and/or tables, authored or reviewed drafts of the article, and approved the final draft.
- Masyitah Zulkifli performed the experiments, authored or reviewed drafts of the article, and approved the final draft.
- Komgrit Eawsakul conceived and designed the experiments, performed the experiments, analyzed the data, prepared figures and/or tables, authored or reviewed drafts of the article, and approved the final draft.
- Tassanee Ongtanasup performed the experiments, analyzed the data, prepared figures and/or tables, authored or reviewed drafts of the article, and approved the final draft.
- Suthinee Sangkanu performed the experiments, authored or reviewed drafts of the article, and approved the final draft.
- Tooba Mahboob analyzed the data, authored or reviewed drafts of the article, and approved the final draft.
- Sonia M.R. Oliveira analyzed the data, authored or reviewed drafts of the article, and approved the final draft.
- Christophe Wiart performed the experiments, authored or reviewed drafts of the article, and approved the final draft.
- Siva Ramamoorthy analyzed the data, authored or reviewed drafts of the article, and approved the final draft.
- Maria de Lourdes Pereira conceived and designed the experiments, authored or reviewed drafts of the article, and approved the final draft.
- Shanmuga Sundar Saravanabhavan analyzed the data, authored or reviewed drafts of the article, and approved the final draft.
- Polrat Wilairatana analyzed the data, authored or reviewed drafts of the article, and approved the final draft.
- Veeranoot Nissapatorn conceived and designed the experiments, authored or reviewed drafts of the article, and approved the final draft.

Data Availability

The following information was supplied regarding data availability:

The raw measurements are available in the Supplemental Files.

Supplemental Information

Supplemental information for this article can be found online at http://dx.doi.org/10.7717/peerj.18452#supplemental-information.

REFERENCES

Al-Enazi NM, Alsamhary K, Ameen F, Nobre MA. 2023. Novel vesicular formulation based on a herbal extract loaded with niosomes and evaluation of its

antimicrobial and anticancer potential. *Microbiology Research* **14**:2133–2147 DOI 10.3390/microbiolres14040144.

Alen Y, Nakajima S, Nitoda T, Baba N, Kanzaki H, Kawazu K. 2000. Antinematodal activity of some tropical rainforest plants against the pinewood nematode, *Bursaphelenchus xylophilus*. *Zeitschrift für Naturforschung. C, A Journal of Biosciences* **55**:295–299 DOI 10.1515/znc-2000-3-425.

Anwar A, Khan NA, Siddiqui R. 2018. Combating *Acanthamoeba* spp. cysts: what are the options? *Parasites & Vectors* **11**:26 DOI 10.1186/s13071-017-2572-z.

Avdagic E, Chew HF, Veldman P, Tu EY, Jafri M, Doshi R, Boggild AK, Reidy JJ, Farooq AV. 2021. Resolution of *Acanthamoeba* keratitis with adjunctive use of oral miltefosine. *Ocular Immunology and Inflammation* **29**:278–281 DOI 10.1080/09273948.2019.1695853.

Barani M, Paknia F, Roostaee M, Kavyani B, Kalantar-Neyestanaki D, Ajalli N, Amirbeigi A. 2023. Niosome as an effective nanoscale solution for the treatment of microbial infections. *BioMed research international* **2023**:9933283 DOI 10.1155/2023/9933283.

Brandt JV, Piazza RD, Dos Santos CC, Vega-Chacon J, Amantea BE, Pinto GC, Magnani M, Piva HL, Tedesco AC, Primo FL, Jafelicci MJ, Marques RFC. 2019. Synthesis and colloidal characterization of folic acid-modified PEG-*b*-PCL micelles for methotrexate delivery. *Colloids and Surfaces B Biointerfaces* **177**:228–234 DOI 10.1016/j.colsurfb.2019.02.008.

Chen L, Han W, Jing W, Feng M, Zhou Q, Cheng X. 2024. Novel anti-*Acanthamoeba* effects elicited by a repurposed poly (ADP-ribose) polymerase inhibitor AZ9482. *Frontiers in Cellular and Infection Microbiology* **14**:1414135 DOI 10.3389/fcimb.2024.1414135.

Chen S, Hanning S, Falconer J, Locke M, Wen J. 2019. Recent advances in non-ionic surfactant vesicles (niosomes): fabrication, characterization, pharmaceutical and cosmetic applications. *European Journal of Pharmaceutics and Biopharmaceutics* **144**:18–39 DOI 10.1016/j.ejpb.2019.08.015.

Chimplee S, Roytrakul S, Sukrong S, Srisawat T, Graidist P, Kanokwiroon K. 2022. Anticancer effects and molecular action of 7-α-hydroxyfrullanolide in G2/M-phase arrest and apoptosis in triple negative breast cancer cells. *Molecules* **27**:407 DOI 10.3390/molecules27020407.

Chuprom J, Kidsin K, Sangkanu S, Nissapatorn V, Wiart C, De Lourdes Pereira M, Wongtawan T, Daus M, Sotthibandhu DS, Tipmanee V, Paul AK, Scholfield CN, Zulkipli MB, Abdullah NH, Mitsuwan W. 2023. Knema retusa is antibacterial and antibiofilm against antibiotic resistant *Staphylococcus aureus* and *S . haemolyticus* isolated in bovine mastitis. *Veterinary Research Communications* **47**:523–538 DOI 10.1007/s11259-022-09999-0.

Chuprom J, Sangkanu S, Mitsuwan W, Boonhok R, Mahabusarakam W, Singh LR, Dumkliang E, Jitrangsri K, Paul AK, Surinkaew S, Wilairatana P, Pereira ML, Rahmatullah M, Wiart C, Oliveira SMR, Nissapatorn V. 2022. Anti-*Acanthamoeba* activity of a semi-synthetic mangostin derivative and its ability in

removal of *Acanthamoeba triangularis* WU19001 on contact lens. *PeerJ* **10**:e14468 DOI 10.7717/peerj.14468.

Eawsakul K, Chinavinijkul P, Saeeng R, Chairoungdua A, Tuchinda P, Nasongkla N. 2017. Preparation and characterizations of RSPP050-loaded polymeric micelles using poly(ethylene glycol)-*b*-poly(epsilon-caprolactone) and poly(ethylene glycol)-*b*-poly(*D. L-lactide)*. *Chemical & Pharmaceutical Bulletin* **65**:530–537 DOI 10.1248/cpb.c16-00871.

El-Nabarawi MA, Abd El Rehem RT, Teaima M, Abary M, El-Mofty HM, Khafagy MM, Lotfy NM, Salah M. 2019. Natamycin niosomes as a promising ocular nanosized delivery system with ketorolac tromethamine for dual effects for treatment of *Candida* rabbit keratitis; *in vitro*/*in vivo* and histopathological studies. *Drug Development and Industrial Pharmacy* **45**:922–936 DOI 10.1080/03639045.2019.1579827.

Fanselow N, Sirajuddin N, Yin X-T, Huang AJW, Stuart PM. 2021. *Acanthamoeba* keratitis, pathology, diagnosis and treatment. *Pathogens* **10**:323 DOI 10.3390/pathogens10030323.

Ge X, Wei M, He S, Yuan WE. 2019. Advances of non-ionic surfactant vesicles (niosomes) and their application in drug delivery. *Pharmaceutics* **11**:55 DOI 10.3390/pharmaceutics11020055.

González-Larraza PG, López-Goerne TM, Padilla-Godínez FJ, González-López MA, Hamdan-Partida A, Gómez E. 2020. IC_{50} evaluation of platinum nanocatalysts for cancer treatment in fibroblast, HeLa, and DU-145 cell lines. *ACS Omega* **5**:25381–25389 DOI 10.1021/acsomega.0c03759.

Gugleva V, Ahchiyska K, Georgieva D, Mihaylova R, Konstantinov S, Dimitrov E, Toncheva-Moncheva N, Rangelov S, Forys A, Trzebicka B, Momekova D. 2023. Development, characterization and pharmacological evaluation of cannabidiol-loaded long circulating niosomes. *Pharmaceutics* **15**:2414 DOI 10.3390/pharmaceutics15102414.

He X, Ji Y, Xie J, Hu W, Jia K, Liu X. 2020. Emulsion solvent evaporation induced self-assembly of polyarylene ether nitrile block copolymers into functional metal coordination polymeric microspheres. *Polymer* **186**:122024 DOI 10.1016/j.polymer.2019.122024.

Hop NQ, Son NT. 2023. Genus *Knema*: an extensive review on traditional uses, phytochemistry, and pharmacology. *Current Pharmaceutical Biotechnology* **24**:1524–1553 DOI 10.2174/1389201024666230201115303.

International Organization for Standardization. 2009. ISO 10993-5 Biological evaluation of medical devices, part 5: tests for in vitro cytotoxicity. Geneva: International Organization for Standardization. *Available at https://www.iso.org/standard/36406.html*.

Kazi KM, Mandal AS, Biswas N, Guha A, Chatterjee S, Behera M, Kuotsu K. 2010. Niosome: a future of targeted drug delivery systems. *Journal of Advanced Pharmaceutical Technology & Research* **1**:374–380 DOI 10.4103/0110-5558.76435.

Kew Royal Botanical Garden. 2023. *Knema retusa* (King) Warb. *Available at https://powo.science.kew.org/taxon/urn:lsid:ipni.org:names:585920-1* (accessed on 12 Febuary 2024).

Kwon GS. 2003. Polymeric micelles for delivery of poorly water-soluble compounds. *Critical Reviews™ in Therapeutic Drug Carrier Systems* **20**:1–47 DOI 10.1615/CritRevTherDrugCarrierSyst.v20.i5.20.

Kot K, Łanocha-Arendarczyk N, Kosik-Bogacka D. 2021. Immunopathogenicity of *Acanthamoeba* spp. in the brain and lungs. *International Journal of Molecular Sciences* **22**:1261 DOI 10.3390/ijms22031261.

Marciano-Cabral F, Cabral G. 2003. *Acanthamoeba* spp. as agents of disease in humans. *Clinical Microbiology Reviews* **16**:273–307 DOI 10.1128/CMR.16.2.273-307.

Matoba A, Weikert MP, Kim S. 2021. Corneal manifestations of miltefosine toxicity in *Acanthamoeba* keratitis. *Ophthalmology* **128**:1273 DOI 10.1016/j.ophtha.2021.06.001.

Miatmoko A, Safitri SA, Aquila F, Cahyani DM, Hariawan BS, Hendrianto E, Hendradi E, Sari R. 2021. Characterization and distribution of niosomes containing ursolic acid coated with chitosan layer. *Research in Pharmaceutical Sciences* **16**:660–673 DOI 10.4103/1735-5362.327512.

Mitsuwan W, Bunsuwansakul C, Leonard TE, Laohaprapanon S, Hounkong K, Bunluepuech K, Kaewjai C, Mahboob T, Sumudi Raju C, Dhobi M, Pereira ML, Nawaz M, Wiart C, Siyadatpanah A, Norouzi R, Nissapatorn V. 2020. *Curcuma longa* ethanol extract and Curcumin inhibit the growth of *Acanthamoeba triangularis* trophozoites and cysts isolated from water reservoirs at Walailak University, Thailand. *Pathogens and Global Health* **114**:194–204 DOI 10.1080/20477724.2020.1755551.

Mitsuwan W, Sin C, Keo S, Sangkanu S, De Lourdes Pereira M, Jimoh TO, Salibay CC, Nawaz M, Norouzi R, Siyadatpanah A, Wiart C, Wilairatana P, Mutombo PN, Nissapatorn V. 2021. Potential anti-*Acanthamoeba* and anti-adhesion activities of *Annona muricata* and *Combretum trifoliatum* extracts and their synergistic effects in combination with chlorhexidine against *Acanthamoeba triangularis* trophozoites and cysts. *Heliyon* **7**:e06976 DOI 10.1016/j.heliyon.2021.e06976.

Nasongkla N, Tuchinda P, Munyoo B, Eawsakul K. 2021. Preparation and characterization of MUC-30-loaded polymeric micelles against MCF-7 cell lines using molecular docking methods and *in vitro* study. *Evidence-Based Complementary and Alternative Medicine : eCAM* **2021**:5597681 DOI 10.1155/2021/5597681.

Ongtanasup T, Kamdenlek P, Manaspon C, Eawsakul K. 2024. Green-synthesized silver nanoparticles from *Zingiber officinale* extract: antioxidant potential, biocompatibility, anti-LOX properties, and *in silico* analysis. *BMC Complementary Medicine and Therapies* **24**:84 DOI 10.1186/s12906-024-04381-w.

Ongtanasup T, Prommee N, Jampa O, Limcharoen T, Wanmasae S, Nissapatorn V, Paul AK, Pereira ML, Wilairatana P, Nasongkla N, Eawsakul K. 2022. The cholesterol-modulating effect of the new herbal medicinal recipe from yellow vine (*Coscinium fenestratum* (Goetgh), ginger (*Zingiber officinale* Roscoe.), and safflower

(*Carthamus tinctorius* L.) on suppressing PCSK9 expression to upregulate LDLR expression in HepG2 cells. *Plants* **11**:1835 DOI 10.3390/plants11141835.

Salleh WMNHW, Ahmad F. 2017. Phytochemistry and biological activities of the Genus *Knema* (*Myristicaceae*). *Pharmaceutical Sciences* **23**:249–255 DOI 10.15171/PS.2017.37.

Salmani-Javan E, Jafari-Gharabaghlou D, Bonabi E, Zarghami N. 2023. Fabricating niosomal-PEG nanoparticles co-loaded with metformin and silibinin for effective treatment of human lung cancer cells. *Frontiers in Oncology* **13**:1193708 DOI 10.3389/fonc.2023.1193708.

Sama-Ae I, Sangkanu S, Siyadatpanah A, Norouzi R, Chuprom J, Mitsuwan W, Surinkaew S, Boonhok R, Paul AK, Mahboob T, Abtahi NS, Jimoh TO, Oliveira SMR, Gupta M, Sin C, de Lourdes Pereira M, Wilairatana P, Wiart C, Rahmatullah M, Dolma KG, Nissapatorn V. 2022. Targeting *Acanthamoeba* proteins interaction with flavonoids of propolis extract by *in vitro* and *in silico* studies for promising therapeutic effects. *F1000 Research* **11**:1274 DOI 10.12688/f1000research.126227.3.

Sangkana S, Eawsakul K, Ongtanasup T, Boonhok R, Mitsuwan W, Chimplee S, Paul AK, Saravanabhavan SS, Mahboob T, Nawaz M, Pereira ML, Wilairatana P, Wiart C, Nissapatorn V. 2024. Preparation and evaluation of a niosomal delivery system containing *G. mangostana* extract and study of its anti-*Acanthamoeba* activity. *Nanoscale Advances* **6**:1467–1479 DOI 10.1039/d3na01016c.

Schuster FL, Guglielmo BJ, Visvesvara GS. 2006. *In-vitro* activity of miltefosine and voriconazole on clinical isolates of free-living amebas: *Balamuthia mandrillaris*, *Acanthamoeba* spp. and *Naegleria fowleri*. *The Journal of Eukaryotic Microbiology* **53**:121–126 DOI 10.1111/j.1550-7408.2005.00082.x.

Sharma G, Kalra SK, Tejan N, Ghoshal U. 2020. Nanoparticles based therapeutic efficacy against *Acanthamoeba*: updates and future prospect. *Experimental Parasitology* **218**:108008 DOI 10.1016/j.exppara.2020.108008.

Shing B, Balen M, McKerrow JH, Debnath A. 2021. *Acanthamoeba* keratitis: an update on amebicidal and cysticidal drug screening methodologies and potential treatment with azole drugs. *Expert Review of Anti-Infective Therapy* **19**:1427–1441 DOI 10.1080/14787210.2021.1924673.

Theerasilp M, Nasongkla N. 2013. Comparative studies of poly(ε-caprolactone) and poly(D. L-lactide) as core materials of polymeric micelles. *Journal of Microencapsulation* **30**:390–397 DOI 10.3109/02652048.2012.746746.

Thulasi P, Saeed HN, Rapuano CJ, Hou JH, Appenheimer AB, Chodosh J, Kang JJ, Morrill AM, Vyas N, Zegans ME, Zuckerman R, Tu EY. 2021. Oral miltefosine as salvage therapy for refractory *Acanthamoeba* keratitis. *American Journal of Ophthalmology* **223**:75–82 DOI 10.1016/j.ajo.2020.09.048.